A Study of an Iris Occlusion Estimation Method

Aniket B. Dharrao[#], Dr. S. R. Ganorkar[*]
[#]*Department of Electronics and Telecommunication, Sinhgad College of Engineering, Vadagaon (Bk), University Of Pune, Pune-411041, India.*
[#]aniket.dharrao11@rediffmail.com
[*]srgomom@rediffmail.com

Abstract- This paper presents a theoretical analysis of an Iris occlusion estimation method. Iris masks play an important role in iris recognition. Iris mask indicate which part of the iris texture map is useful and which part is occluded (contaminated) by noisy image artifacts such as eyelashes, eyelids, eyeglasses frames and specular reflections. The accuracy of an iris mask plays an important role in iris recognition system. The performance of recognition system decreases when iris mask is inaccurate even if best recognition algorithm is used. We propose to use Figueiredo and Jain's Gaussians mixture models (FJ-GMMs) to model the underlying probabilistic distributions of both valid and invalid region in iris images.

Keyword: Figueiredo and Jain's Gaussians mixture models (FJ-GMMs), Gabor Filter, Simulated Annealing.

I. INTRODUCTION

Iris recognition is a particular type of biometric system that can be used to reliably indentify a person by analyzing the patterns found in the iris. The iris is so reliable as a form of identification because of the uniqueness of its pattern.
In most cases, after transforming iris texture from the Cartesian coordinate to the polar coordinate, one has to create a mask for the iris map in the polar coordinate. The goal of this mask is to indicate which part in the iris map is truly iris texture and which part is noise. The occlusion artifacts of the iris map may consist of eyelids, eyelashes, shadows, or specular reflections.

Fig.1: Normalization iris texture map (upper picture) and its accurate mask (lower picture), with white color indicating occluded area [1]

Fig. 1 shows example images of an iris texture map and its accurate mask. Note that in the iris texture, the noisy regions consist of artifacts created by eyelids, eyelashes, and specular reflections. All of these noise artifacts have to be indicated in the mask in order to be ignored in the spatial feature match process in order to achieve the highest performance of iris recognition. The accuracy of the iris masks has a great impact on the recognition accuracy of the iris recognition systems. The main focus of iris recognition research addresses the power of the matching algorithm and the feature extraction. However, if the iris masks are inaccurate, the best feature extraction and recognition algorithms cannot compensate for such flaws. The overall recognition rate will decrease dramatically because the region of the invalid iris is used during feature extraction and matching.

A. Iris Recognition System

Iris Recognition is a rapidly expanding method of biometric authentication that uses Pattern-recognition techniques on images of irides to uniquely identify an individual.

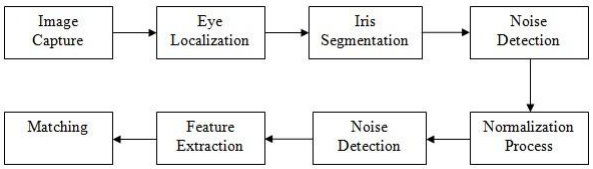

Fig.2: Iris Recognition System Block Diagram [1]

Image Capture: To capture the rich details of iris patterns, an imaging system should resolve a minimum of 70 pixels in iris radius.
Image Localization: Before recognition of iris takes place, the iris is located using landmark features. These landmark features and distinct shape of the iris allow for imaging, feature isolation and extraction
Iris Segmentation: Apply curve fitting technique to detect inner and outer boundaries of the iris and upper and lower eyelids. Then, implement the proposed noise detection method to segment the eyelashes and reflection.
Iris Normalization: In most cases, in the iris normalization stage, iris images are transformed from the Cartesian coordinate system to the polar coordinate system known as unwrapping process.

II. OVERVIEW OF WORK

Daugman's work is one of the earliest in iris recognition [2]. In 1993, he described the normalization scheme for iris texture, calling it the "Doubly Dimensionless Projected Polar Coordinate System in which assumes the top part of the image and the 45 degree notch at the 6 o'clock position are occluded for every iris image.

Ma et al. proposed a full framework for an iris recognition system [4].They merely stated that they discarded the lower part of the normalized iris texture and focused only on the more discriminative regions. A similar assumption was proposed in the work of Tisse et al. [5].

Daugman, in a later work, proposed a more sophisticated algorithm for finding occluded regions in the iris images [3].By replacing the circular integration operator with the spline parameter, one can approximately locate the eyelid boundaries. Furthermore, in his latest work [6], he proposed a new method which uses active contours to find the boundary of the eyelids.

Kong and Zhang proposed a model for detecting eyelashes and specular reflections [9]. They proposed using Gabor filters to detect separable eyelashes and used the variance of intensity in the local window to locate clusters of multiple eyelashes.

Zou et al. proposed a procedure for iris occlusion estimation [10]. It consisted of four stages: First, they detected the horizontal edges of the eyelids. Second, they performed morphological operations on those edges to enhance them. Third, they used the segmentation result to localize valid edge candidates. Finally, they used connectivity information to refine the mask.

In [7], Krichen et al. proposed a probabilistic approach for iris quality measure. The iris masks estimated by their method seem to be local patch-based, not pixel-based. In [8], Thornton proposed using a discriminative learning method based on Fisher Linear Discriminant Analysis (FLDA) to estimate iris masks in the polar domain.

In [11], Tsai et al. perform Gabor filter optimization with particle swarm technique for the purpose of iris recognition.

III. PROPOSED METHOD

To overcome the shortcomings of previous methods, we suggest a method for automatic iris mask generation. This method has to be flexible for all possible sizes of iris images. It should be capable of co working with various iris acquisition devices across different optical sensors. Existing methods like rule-based type would definitely not be able to achieve such a goal. Therefore, we propose a learning-based approach to solve this problem, which is a new perspective to looking at the problem.

A. A Recognition Perspective to the Problem

The problem of generating a mask for an iris map can be seen as a two-class classification problem. Given an input of an iris texture map in normalized form (denoted by I, and we assume the size of the iris map is *M X N*), the output should be another binary image (denoted by Mask) of the same size on which every pixel is either of value 0 or 1. A binary value 0 appearing on Mask (I, j) means that the pixel at the location I(I, j) belongs to the "valid" iris region (authentic iris texture), and 1 the occluded region (eyelash, eye, specular reflection, etc.).

Gaussian Mixture Model

A Gaussian Mixture Model (GMM) is a parametric probability density function represented as a weighted sum of Gaussian component densities as given by the equation,

$$p(X|\lambda) = \sum_{i=1}^{M} \text{Wi } g(X|\mu i, \Sigma i) \quad (1)$$

Where X is a D-dimensional continuous-valued data vector, Wi, i = 1. . . M, are the mixture weights, and g (X|μi, Σi), i = 1. . . M, are the component Gaussian densities. Each component density is a D-variate Gaussian function of the form,

$$g(X|\mu i, \Sigma i) = \frac{1}{2\pi^{\frac{D}{2}}|\Sigma i|^{0.5}} \exp\left\{-\frac{1}{2}(X-\mu i)' \sum_i^{-1}(X-\mu i)\right. \quad (2)$$

with mean vector μi and covariance matrix Σi. The mixture weights satisfy the constraint that $\sum_{i=1}^{M} Wi = 1$.

For the choices of the classifier, we propose the use of a Gaussian Mixture Modeling (GMM) to model the posterior probability distribution of both iris texture and occlusion regions. As long as the number of Gaussians is large enough, GMM can model virtually any distribution. Another advantage of GMM is that its mathematical equation is easy to evaluate; thus the classification speed is very high during the test stage.

The training of GMM uses Expectation-Maximization (EM) to optimize the parameters for Gaussian mixtures. EM-based parameter estimation for GMM training has a few drawbacks. Due to these major drawbacks in EM training algorithm, we decided to use an alternative training approach. Figueiredo and Jain proposed an unsupervised learning method for training GMMs [12]. This method can estimate the number of Gaussian mixtures without human intervention, and can avoid the boundary of the parameter space during the converging stage. The basic idea of Figueiredo-Jain's extension for GMM training (FJ-GMM algorithm) is that it dynamically adjusts the number of Gaussians by eliminating Gaussians which are not supported by the observation. The details of FJ-GMM training can be found in [12].

B. Feature Set Exploration

In the second stage, we focus on fine-tuning the feature set used for classification. As we know GMM can model data distribution in high dimensional space.

Fig .3: The Feature sets (textons) used in experiment of feature set exploration [1].

We use a few basic features which are very popular in image processing.

1. The X and Y coordinate of the pixel: Since the way of normalizing an iris image from Cartesian coordinate to polar coordinate is consistent, we expect that the location where the eyelid and eyelashes in the training and test set should be close.
2. The pixel value (denoted by I).
3. The mean and the standard deviation in a local 3X3 neighborhood, denoted by M and S, respectively.
4. Response intensity after the image is filtered by the Sobel edge filter.
5. Response intensity after the image is filtered by Laplacian of Gaussian (LoG), denoted by L.
6. Response intensity after the image is filtered by Gabor filter, denoted by G.

Fig.3 gives a visual illustration of the entire feature sets used.

C. Parameter Optimization for Gabor Filters

After studying all results, we conclude Gabor filter is the best to extract the important features for goal of classification between iris texture and occlusion artifacts.

1. Optimization for Single Gabor Filter

The mathematical equation of the generic Gabor filter is given below:

$$g(x,y;\lambda,\Theta,\psi,\gamma) = e^{-\frac{x'^2+\gamma^2 y'^2}{2\sigma^2}}\cos\left(2\pi\frac{x'}{\lambda}+\psi\right) \quad (3)$$

Where x' = xcosθ+ysinθ and y'=-xsinθ+ycosθ. In this equation, λ represents' the wavelength of wavelet, θ is the in-plane rotational angle of filter, ψ is the phase offset between the peak and valley of the wavelet, γ is the aspect ratio and it specifies the elipticity of support of Gabor function, σ specifies the variance.

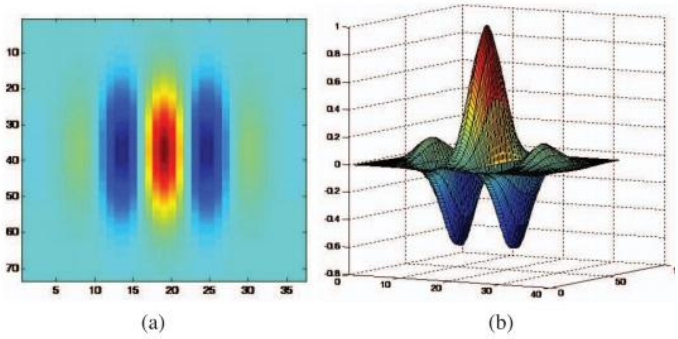

Fig.4: Example of a Gabor filter. (a) 2D view. (b) 3D view [1].

Intuitively, our goal should be discovering ĝ so that

$$\hat{g} = arg \min_{\{\lambda,\theta,\psi,\sigma,\gamma\}} AER\ (g(x,y;\lambda,\theta,\psi,\sigma,\gamma)) \quad (4)$$

Where AER () is a function that returns the Average Error Rate of the iris mask, given that we use the Gabor filter g () to extract features. That means we are not using (4) as our objective function. Instead, we are using this formula:

$$\hat{g} = arg \min_{\{\lambda,\theta,\psi,\sigma,\gamma\}} FRR0.1\ (g(x,y;\lambda,\theta,\psi,\sigma,\gamma)) \quad (5)$$

Where FRR0.1 stands for the False Reject Rate (FRR) when the False Accept Rate (FAR) equals 0.1 percent.

The step to compute ĝ is as follows:

1. Given a specific set of Gabor parameter (x, y; λ, θ, ψ, σ, γ), use the corresponding Gabor filter to extract a feature from the iris images of training set.
2. Use the feature set (consisting of pixel location, pixel intensity, and response from Gabor) to train GMM, with FJ-GMM training algorithm.
3. Estimate the iris occlusion map for every image in the test set.
4. Perform large-scale iris recognition using iris images and estimated occlusion map in the test set, then compute FRR at FAR=0.1percent.
5. Use the result in step 4 as the output of cost function, then go back to step 1 .

In step 4, we choose to use Simulated Annealing (SA) method as our optimization algorithm. SA is a stochastic global optimization method which can

1. process cost functions
2. process arbitrary boundary conditions and constraints imposed on those cost functions;
3. be implemented quite easily with minimal effort of coding;
4. Statistically finds of an optimal solution.

2. Optimization for Gabor Filter Banks

Gabor filter banks, that maximizes the performance of proposed algorithm.GFB can be defined as

$$GFBN = \{\hat{g}1, \hat{g}2, \ldots..\hat{g}N\} \quad (6)$$

Where N denotes number of Gabor filters for GFB.

Training procedure is described as follows:

1. Estimate $\hat{g}_1$ by using (5), and set $GFB_1 = \{\hat{g}_1\}$.
2. Set N as maximal number of Gabor filter we would like to discover.
3. When i < N, repeat the following steps:
   a) Estimate $\hat{g}_{i+1}$ by $\hat{g}_{i+1} = \arg\min_{gj} FRR0.1\ (g_j(x,y;\lambda,\theta,\psi,\sigma,\gamma)|GFB_i)$.This optimization process is achieved by simulated annealing method.
   b) Set $GFB_{i+1} = GFB_i \cup \hat{g}_{i+1} = \{\hat{g}_1, \hat{g}_{2,\ldots\ldots} \hat{g}_{i+1}\}$.

IV. REVIEWED RESULTS

A. GMM Trained on Single Image

We first try suggested method on a single iris image to see how the trained GMM would fit into the training data. Taking the image 1.giff from the ICE2 database to be our training sample. After manually segmenting the iris and performing iris normalization, we get Fig. 5a. Because we used the intensity value of every pixel as the Z coordinate of each pixel in three-dimensional space, we were able to plot the iris texture map in Fig. 5a in a 3D perspective, as shown in

Fig. 5b. Fig. 5a to indicate which part was valid iris texture to use this information as the class labels for each pixel. After manually creating the iris masks, we assign the class label to each pixel. These pixels, together with their labels, form the training dataset, which was then used to train two GMM models; the first one modeled the distribution of the valid iris texture, and the second one the occluded regions. The plot of the trained GMMs is shown in Fig. 6c. In Fig. 6c, GMMs with the red color represent GMMs trained for occlusion, and GMMs with the green color are models for iris texture.

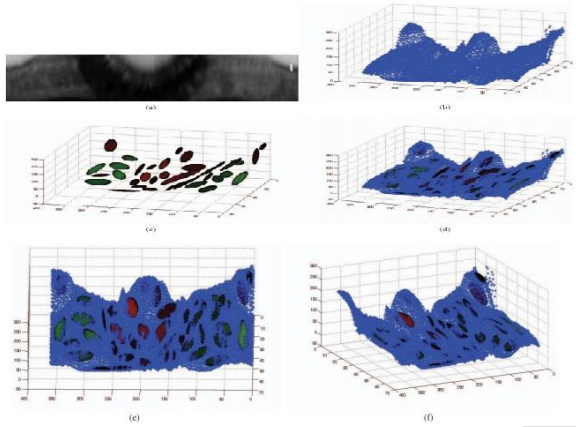

Fig.5: Visualization of GMM trained on single iris texture [1].

In Figs. 5d, 5e, and 5f plotted the trained GMMs together with all pixel values in 3D space. The red GMMs modeled the noisy parts, while the green GMMs modeled the valid iris texture area.

If we use Fig. 5a as our test image and use the trained GMM to perform the classification for every pixel on this image, plotting the results of the classification back into a two-dimensional array, with 0 indicating the valid iris and 1 indicating the occlusion region, we can visualize the mask generated by the GMM. We show the comparison of the iris mask estimated by different algorithms in Fig. 7. The input iris texture image in the polar coordinate is shown in Fig. 7a, while the ground truth of the mask, shown in Fig. 7b, is manually labeled. The mask generated by the proposed method is shown in Fig. 3.3d, compared with another mask generated by a rule-based method,

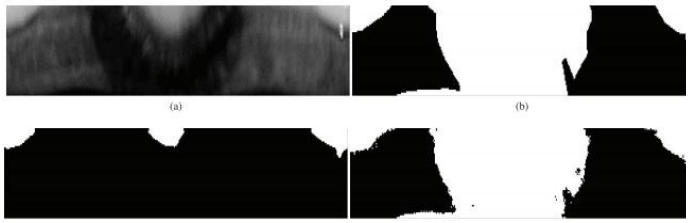

Fig.6: Comparison of the iris mask estimated by different algorithms [1].

shown in Fig. 6c. As we can see, the result generated by the proposed algorithm is much better than what we can get using the rule-based method.

B. Feature Set Exploration

In order to organize the experimental process and results, we gave a code name to each experiment in order to better distinguish what we tried in each experiment. The code names and the features are listed below.

1. SxSyL: Response intensity after the image is filtered by Sobel edge
2. IG: Intensity of the pixel and response intensity after the image is filtered by Gabor filter.
3. IMSSxSyLG: Combination of all above.

The first baseline method we used is the rule-based method, which detects whether there is a strong variance of pixel intensity in a local window and uses it as a feature for classification.

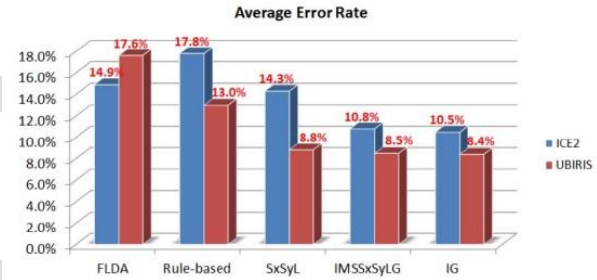

Fig.7 The average error rate for the mask estimated by different algorithms [1].

For a fair comparison, the second baseline method used the Fisher Linear Discriminant Analysis to perform classification, as opposed to our generative approach (GMM). In this method, the feature set includes:

1. Local mean
2. Local standard deviation
3. A ratio that tells the percentage of pixel in a local window for which the LSD is greater than the global mean.
4. The position of pixel.

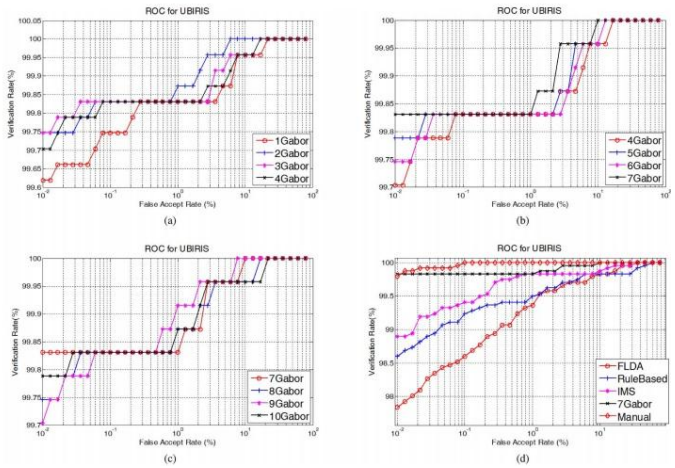

Fig.8: ROC curves show that how the recognition rate changes with the number of filters in GFB with the UBIRIS database [1]

For each iris class in ICE2 and UBIRIS, we picked one image as training data and left all the other images as test data.

For each testing image, we computed the Average Error Rate of the masks. AER can be computed as

$$AER = \frac{\sum_{i=1}^{N} e_i}{N} \quad (7)$$

$$e_i = \frac{NP(mask_{alg} \otimes mask_{gt})}{W\ X\ H} \quad (8)$$

Where (W, H) is the size of the mask, $mask_{alg}$ and $mask_{gt}$ the masks generated by specified algorithm and human labor respectively, N is the total number of test images, $\otimes$ the pixel-wise XOR operator that used to compute the difference between two occlusion masks, NP() is the function that counts the number of pixels in an image which are not zeros. From the results shown in Fig. 8, for the feature set selection, we found that the feature set IG performs better than other combinations. Therefore, the image response generated by Gabor filtering is much more discriminative than those generated by other filters (Sobel, Gaussian, and Laplacian of Gaussian). Fig. 9 shows the same results for the ICE2 database.

E. DISCUSSION

1. Average Error Rate for Occlusion Estimation

In terms of the accuracy of the generated iris mask, Fig. 8 shows that in both the ICE2 and UBIRIS database, our proposed method is better than the two baseline methods.

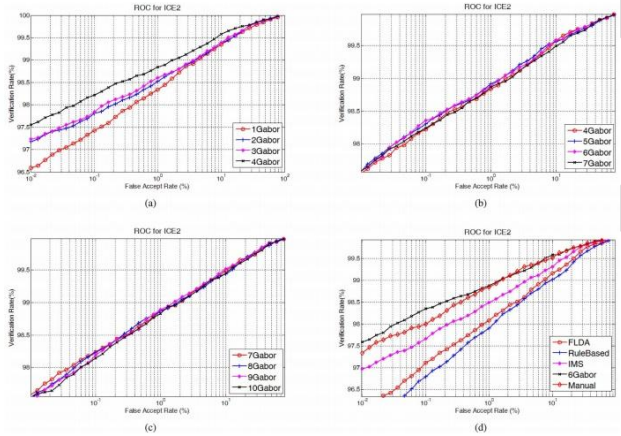

Fig.9: ROC curves that show how the recognition rate changes with the number of filters in GFB with the ICE2 database. [1].

From Fig. 8 we found that feature IG seems to give the best result among all the feature combinations.

2. Gabor Filter Bank Optimization

For the UBIRIS database, as the number of Gabor filters increases, we find that the recognition performance also increases. However, the improvement of performance seems to saturate at the point when seven Gabor filters are used.

When more than seven Gabor filters are used, the ROC curve begins to drop down, as shown in Fig. 9c. We thus conclude that, though multiple Gabor filters can give the most discriminative feature for occlusion estimation, there is a limit. This same phenomenon can be observed in the case of the ICE2 database, as shown in Fig. 9. For ICE2, the optimal number of Gabor filters is six.

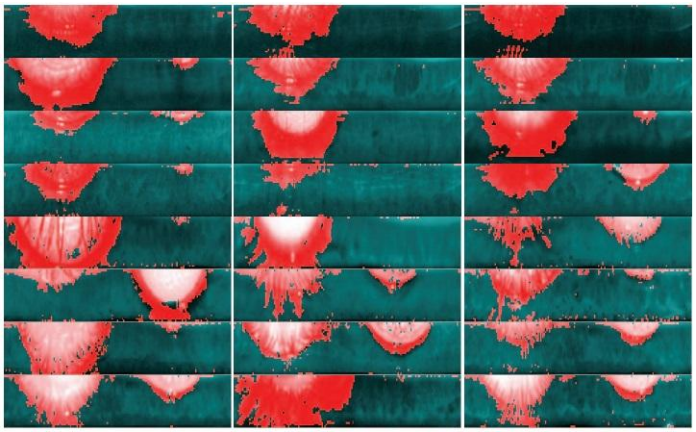

Fig.10: Iris occlusion estimated by the proposed algorithm. [1]

3. Gabor Filters that are learned in Experiments

Figs. 8b and 9b show the Gabor filters that are learned during the optimization process. For the ICE2 database, the quality of images is very good; therefore most iris texture regions are sharp and clear. The appearance of learned Gabor is close to the primitive form.

The Gabor filters learned for UBIRIS look a bit different. Since images in UBIRIS are noisy, the shape of the learned Gabor filter looks very complex. In this case, FJ-GMM is doing more work of learning texton about an invalid iris region.

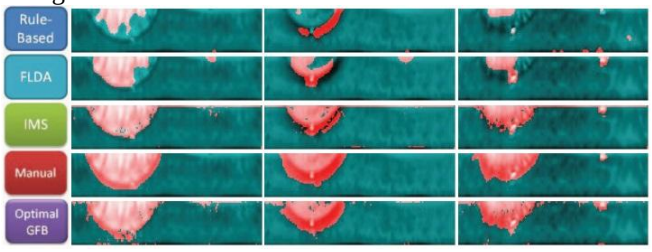

Fig.11: Comparison of the iris masks that are estimated by different algorithms [1].

4. Comparison with previous works

Basically, SA can be thought as GA where the population size is only one. SA creates a new solution by randomly choosing a new candidate in the neighborhood, but GA creates solutions by combining two different solutions.

Practically speaking, in our problem the bottleneck of computation is related to evaluating the cost function. It seems that SA can converge to a better solution in a shorter time compared to GA .Therefore, in our proposed method, using SA for Gabor filter optimization is an appropriate choice.

5. Actual Simulation Results

The pupil in the acquired image usually contains reflection from the source, which form some bright spots in the pupil, so if the pixel value inside the pupil is over a particular threshold (200) then it is replaced by pixel value of some neighborhood pixel. This operation almost fills the circles. The original image along with ROI marked pupil boundary, iris boundary, occluded part is shown in following fig. 12 (a) and (b).

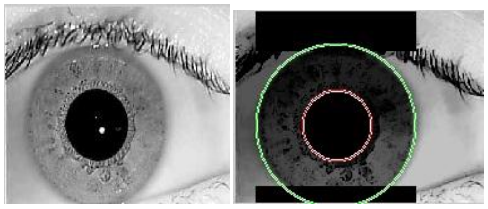

Fig.12 :(a) Original gray scale image. (b) ROI marked with pupil and iris boundary with internal reflection removed.

The final ROI with enhanced normalized image is shown in fig.13 which is the final output of Daugman rubber sheet model.

Fig.13: Normalized final ROI

V. CONCLUSION

Estimation of iris mask robustly is one of the key factors to achieve high iris recognition rates. First formulation of the problem with pattern-recognition framework and propose a generative model to solve it. Secondly, search for feature set that is best of image intensity and response of Gabor filter is the best feature set. Third, optimization of the parameters for GFB in order to recover the 10 Gabor filters that are best suits for our goal. The experimental results show that proposed method can detect the occluded regions in an iris in polar form. Fourth, the proposed method only needs to use single training image from each class to get a satisfactory result for estimating iris masks. This is one of the very useful features in consideration of practical scenario.

REFERENCES

[1] Yung-Hui Li, Marios Savvides "An Automatic Iris Occlusion Estimation Method Based on High-Dimensional Density Estimation", *IEEE Transactions on Pattern Analysis and Machine Intelligence, Vol. 35, No. 4, April 2013, Pp.784*

[2] J. Daugman, "High Confidence Visual Recognition of Persons by a Test of Statistical Independence*," IEEE Trans. Pattern Analysis and Machine Intelligence, vol. 15, no. 11, pp. 1148-1161, Nov. 1993.*

[3] J. Daugman, "How Iris Recognition Works," *Proc. Int'l Conf. Image Processing, vol. 1, pp. I-33-I-36, 2002.*

[4] L. Ma, T. Tan, Y. Wang, and D. Zhang, "Personal Identification Based on Iris Texture Analysis," *IEEE Trans. Pattern Analysis and Machine Intelligence, vol. 25, no. 12, pp. 1519-1533, Dec. 2003.*

[5] C. Tisse, L. Martin, L. Torres, and M. Robert, "Person Identification Technique Using Human Iris Recognition,"*citeseer.ist.psu. edu/tisse02person.html, 2002.*

[6] J. Daugman, "Biometric Personal Identification System Based on Iris Analysis," *US Patent 291560, 1994.*

[7] E. Krichen, S. Garcia-Salicetti, and B. Dorizzi, "A New Probabilistic Iris Quality Measure for Comprehensive Noise Detection," *Proc. First IEEE Int'l Conf. Biometrics: Theory, Applications, and Systems, pp. 1-6, Sept. 2007.*

[8] J. Thornton, "Matching Deformed and Occluded Iris Patterns: A Probabilistic Model Based on Discriminative Cues," *PhD thesis, Dept of Electrical and Computer Eng., Carnegie Mellon Univ., 2007.*

[9] W. Kong and D. Zhang, "Accurate Iris Segmentation Based on Novel Reflection and Eyelash Detection Model," *Proc. Int'l Symp.Intelligent Multimedia, Video, and Speech Processing, pp. 263-266, 2001.*

[10] J. Zuo, N. Kalka, and N. Schmid, "A Robust Iris Segmentation Procedure for Unconstrained Subject Presentation," *Proc. Special Session on Research at the Biometric Consortium Conf. Biometrics Symp., pp. 1-6, Aug. 21-Sept. 19, 2006.*

[11] C. Tsai, J. Taur, and C. Tao, "Iris Recognition Using Gabor Filters Optimized by the Particle Swarm Technique", *Proc. IEEE Int'l Conf. Systems, Man, and Cybernetics, pp. 921-926, Oct. 2008.*

[12] M. Figueiredo and A. Jain, "Unsupervised Learning of Finite Mixture Models,"*IEEE Trans. Pattern Analysis and Machine Intelligence, vol. 24, no. 3, pp. 381-396, Mar. 2002*

[13] Arun Passi, Ajay Kumar,"Improving Iris Identification using User Quality and Cohort Information", *IEEE Trans. Dec. 2007.*